

A New Type of Metalloprotein: The Mo Storage Protein from *Azotobacter vinelandii* Contains a Polynuclear Molybdenum–Oxide Cluster

Dirk Fenske,^[a] Manuel Gnida,^[b, c] Klaus Schneider,^[a] Wolfram Meyer-Klaucke,^[b] Jörg Schemberg,^[a] Volker Henschel,^[a] Anne-Katrin Meyer,^[d] Arndt Knöchel,^[d] and Achim Müller*^[a]

Dedicated to Professor Dr. Rüdiger Kniep on the occasion of his 60th birthday

Azotobacter vinelandii is a diazotrophic bacterium characterized by the outstanding capability of storing Mo in a special storage protein, which guarantees Mo-dependent nitrogen fixation even under growth conditions of extreme Mo starvation. The Mo storage protein is constitutively synthesized with respect to the nitrogen source and is regulated by molybdenum at an extremely low concentration level (0–50 nM). This protein was isolated as an $\alpha_4\beta_4$ octamer with a total molecular mass of about 240 kg mol⁻¹ and its shape was determined by small-angle X-ray scattering. The genes of the α and β subunits were unequivocally identified;

the amino acid sequences thereby determined reveal that the Mo storage protein is not related to any other known molybdoprotein. Each protein molecule can store at least 90 Mo atoms. Extended X-ray absorption fine-structure spectroscopy identified a metal–oxygen cluster bound to the Mo storage protein. The binding of Mo (biosynthesis and incorporation of the cluster) is dependent on adenosine triphosphate (ATP); Mo release is ATP-independent but pH-regulated, occurring only above pH 7.1. This Mo storage protein is the only known noniron metal storage system in the biosphere containing a metal–oxygen cluster.

Introduction

The uptake, processing, and storage of metals in organisms, from mammals to microorganisms, has attracted the interest of scientists from different fields, for example, bioinorganic chemistry, genetics, medicine, and ecology. A specially fascinating case is the complex Mo metabolism in N₂-fixing bacteria which has been particularly extensively investigated for *Azotobacter vinelandii*.^[1] Correspondingly, several proteins involved in this metabolism have been thoroughly characterized; most of them are members of the “molbindin” family (Mop and Mod proteins), share a common “Mop motif” in their amino acid sequence, and contain Mo in the form of monomeric molybdate anions.^[2]

In *A. vinelandii*, an aerobic bacterium that is widespread in soils and waters, another Mo protein exists, designated as the “molybdenum storage protein” (MoSto), which is functionally connected to nitrogen fixation^[3] and enables the accumulation of enormous amounts of Mo inside the cell,^[3–5] thus supplying the conventional nitrogenase system with Mo even in an Mo-deficient environment. The bioavailability of Mo in soils is highly variable and may easily become a growth-limiting factor for nitrogen-fixing bacteria. It has been observed that even in habitats where some Mo is available, the growth of N₂-fixing organisms may cause a self-produced Mo starvation in the surrounding environment.^[6] Due to its high Mo uptake activity, *A. vinelandii* has even been used to remove molybdate from liquid growth media, thus very rapidly (within 10–15 min) creating almost Mo-free nutrient solutions which are used for de-repression of the Fe nitrogenase system in *Rhodobacter capsu-*

latus.^[4] It is therefore clear that in natural habitats, where organisms compete for molybdate ions, species like *A. vinelandii*, equipped with such a high-capacity storage system that scavenges Mo very effectively from the close environment, will certainly have a great selective advantage.

Remarkably, despite the obvious physiological and ecological importance of MoSto, research into this protein has been neglected so far. Since its first isolation and basic characterization more than 20 years ago,^[3] no further detailed publication has followed. The only attempt ever to obtain information about the nature of the protein-bound Mo was based on time-differential perturbed angular correlation of γ rays (TDPAC)

[a] D. Fenske,⁺ Dr. K. Schneider, J. Schemberg, V. Henschel, Prof. A. Müller
Lehrstuhl für Anorganische Chemie I, Universität Bielefeld
Universitätsstrasse 25, 33615 Bielefeld (Germany)
Fax: (+49) 521-106-6003
E-mail: a.mueller@uni-bielefeld.de

[b] Dr. M. Gnida,⁺ Dr. W. Meyer-Klaucke
European Molecular Biology Laboratory, Outstation Hamburg
DESY Building 25A, Notkestrasse 85, 22603 Hamburg (Germany)

[c] Dr. M. Gnida⁺
Current address:
NMR Department, Bijvoet Center for Biomolecular Research
Utrecht University, Bloemberggebouw
Padualaan 8, 3584 CH Utrecht (The Netherlands)

[d] A.-K. Meyer, Prof. A. Knöchel
Institut für Anorganische und Angewandte Chemie, Universität Hamburg
Martin-Luther-King-Platz 6, 20146 Hamburg (Germany)

[*] These authors contributed equally to this work.

measurements with ^{99}Mo described by Müller et al.^[5] Despite the limitations of this method (yielding a fingerprint only, no explicit structural information like interatomic distances, bond angles, etc.) and the fact that the experiments were done only with whole cells and cell-free extracts, and not with purified protein, the TDPAC spectra gave the first hint that the Mo component in MoSto might be a polynuclear metal–oxygen cluster.^[5] The iron storage proteins ferritin^[7] and frataxin^[8,9] are currently the only reported examples of biological metal storage in the form of such a cluster.

The work presented herein is the first comprehensive biochemical characterization of MoSto, including data on the Mo-binding/release mechanism, identification of the encoding genes, determination of the protein shape by means of small-angle X-ray scattering (SAXS) analysis, and characterization of the protein-bound Mo component by using extended X-ray absorption fine-structure (EXAFS) spectroscopy.

Results and Discussion

Purification of MoSto, molecular mass, subunits, and Mo content

The purification protocol described in the literature^[3] has been improved. As summarized in Table 1, DEAE–Sephacel anion-exchange chromatography was applied as the first step and was followed by ammonium sulphate fractionation (40–50% saturation) and gel filtration on Superdex 200; this resulted in MoSto preparations which were >95% pure according to electrophoretic analyses (Figure 1 A).

Table 1. Purification of MoSto.

Preparation	Volume [mL]	Total Mo [μmol]	Total protein [mg]	Mo/protein [$\mu\text{mol g}^{-1}$]	Mo recovery [%]
crude extract	20	9.6	570	16.8	100
DEAE–Sephacel peak fractions	40	4.9	36	136	51
ammonium sulphate precipitate (50%)	0.9	2.2	15	147	23
Superdex 200 peak fractions	25	1.2	4.2	286	12.5

The crucial improvement in this procedure was the use of Superdex 200 as the gel filtration material. Sephadex G-100 had been applied in the first, and so far only, isolation of MoSto more than 20 years ago.^[3] Due to its fractionation range of 4–150 kg mol^{-1} , that material is definitely not suitable for the separation and molecular-mass determination of proteins of the size of MoSto. On Sephadex G-150 (fractionation range: 5–300 kg mol^{-1}), Sephadex G-200 (5–600 kg mol^{-1}), and Superdex 200 (10–600 kg mol^{-1}) columns, MoSto eluted at a point corresponding to a molecular mass of about 240 kg mol^{-1} , while a molecular mass of 247 kg mol^{-1} was determined independently from SAXS data by reference to a standard sample of bovine serum albumin.

SDS-PAGE results proved that MoSto consists of equal amounts of two different subunits (Figure 1 A), for which matrix-assisted laser desorption/ionization time-of-flight

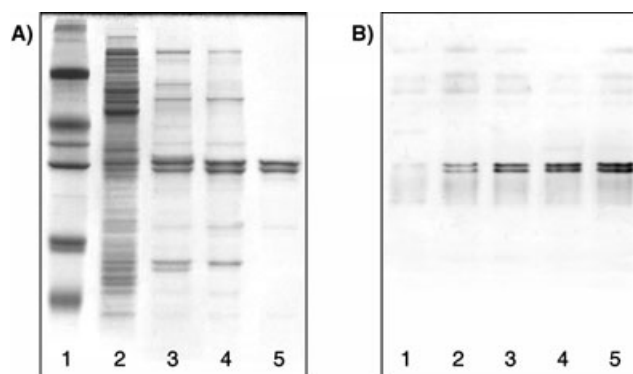


Figure 1. A) Sodium dodecylsulfate polyacrylamide gel electrophoresis (SDS-PAGE; tris(hydroxymethyl)aminomethane (Tris)/glycine buffer system, Coomassie staining) of solutions from different steps of MoSto purification. Lane 1: molecular mass marker, with bands at 66, 45, 36, 29, 20 and 14 kg mol^{-1} . Lane 2: crude cell-free extract. Lanes 3–5: protein solution after diethylaminoethyl (DEAE) chromatography (3), ammonium sulphate fractionation (4), and gel filtration (5). MoSto forms a characteristic double band at approx. 29 kg mol^{-1} .

B) Western immunoblot analysis of the influence of molybdate concentration on MoSto expression. The intensity of the twin bands representing the α and β subunits of MoSto increases with increasing $[\text{MoO}_4]^{2-}$ concentration. The concentrations used in the cultures were: lane 1: no added $[\text{MoO}_4]^{2-}$; lane 2: 1 nM $[\text{MoO}_4]^{2-}$; lane 3: 2 nM $[\text{MoO}_4]^{2-}$; lane 4: 10 nM $[\text{MoO}_4]^{2-}$; lane 5: 50 nM $[\text{MoO}_4]^{2-}$.

(MALDI-TOF) mass spectrometry on a purified sample yielded masses of 29.12 (α subunit) and 28.15 kg mol^{-1} (β subunit). This demonstrates that the functional protein is an $\alpha_4\beta_4$ octamer rather than an $\alpha_2\beta_2$ tetramer (90 kg mol^{-1}) with subunit masses of 21 and 24 kg mol^{-1} , as assumed by Pienkos and Brill.^[3] MoSto molecules present in a tetrameric state have never been found to exist in our preparations.

The most important criterium for a successful purification on the one hand and for the intactness and quality of the native storage protein on the other hand is certainly the Mo content of the isolated protein. The Mo content of MoSto was, depending on the preparation conditions, highly variable. In samples from purifications with Sephadex G-200 as the gel filtration material, values of 30–45 Mo atoms per protein molecule (125–190 μmol of Mo per gram of protein) were typically obtained. This corresponds to the Mo content reported by Pienkos and Brill,^[3] who determined 14.5 atoms per MoSto molecule based on an assumed protein mass of only 90 kg mol^{-1} . It is pertinent to note that we sometimes obtained higher Mo-to-protein ratios with less pure samples from early stages of the purification than with the final pure product, a fact indicating that, at least during the final gel filtration step, a certain proportion of Mo was lost. The Mo loss could be prevented to a great extent by changing the gel filtration medium from Sephadex G-200 to Superdex 200, thus avoiding extensive dilution of the protein solution and speeding up the whole purification to fit it into one day (15 h). This

procedure (see the Experimental Section) yielded samples with up to 70 Mo atoms per molecule ($292 \mu\text{mol g}^{-1}$). However, even then, a loss of at least 23% of the bound Mo in a low-molecular-weight form could be observed, from which an Mo content of approximately 90 atoms per molecule can be estimated for the MoSto preparation prior to the Superdex step. The real Mo storage capacity of MoSto might even be higher. A similar variability in metal content has been reported for the Fe storage system ferritin. Isolated ferritins carry 800–2500 metal atoms, a value corresponding to approximately 15–55% of the maximum load.^[7]

Molecule shape and amino acid sequence

The shape of MoSto was calculated *ab initio* with a resolution of approximately 20 Å by using SAXS data. Although no symmetry constraints were imposed on the calculations, the resulting models indicate not a spherical, but an elongated molecule (about 12 nm long) with twofold symmetry (Figure 2). It is therefore conceivable that MoSto might be a dimer of $\alpha_2\beta_2$ tetramers that results in an octameric ($\alpha_2\beta_2$)₂ subunit arrangement.

The subunits were separated by SDS-PAGE and sequences of about 30 amino acids each could be determined from their N-termini. These starting sequences match the products of the *or5808* and *or5807* genes in the *Azotobacter* Genome Project database.^[10] Those genes code peptide chains with molecular masses of 29188 g mol^{-1} and 28225 g mol^{-1} , which agree with our mass spectrometry results. We propose to name those genes coding the α and β subunits of MoSto, *mosA* and *mosB*, respectively. The complete amino acid sequences as translated from the genome are given in Figure 3. The subunits are related to each other (42% identical residues) and probably evolved from a duplicated single gene.

Interestingly, the so-called Mop unit is not present in MoSto. The Mop unit is a well-conserved single-molybdate-binding domain of about 70 amino acids, which is common to bacterial proteins involved in Mo transport (for ex-

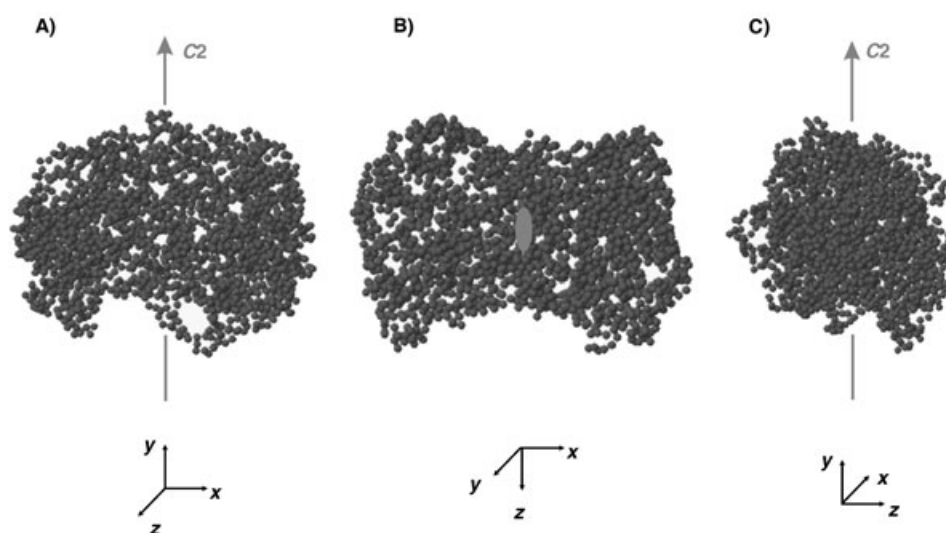


Figure 2. The shape of MoSto determined *ab initio* by SAXS analysis in three different views. As indicated, the molecule appears to have a twofold symmetry (C_2 axis).

ample, ModC), Mo-dependent gene regulation (ModE), and intracellular Mo-concentration buffering (ModG and the Mop proteins).^[2,11] On comparing the MoSto sequences with those of the Mop domains of 13 different molybdate-binding proteins,^[11] no satisfactory alignment with either of the two subunits could be found.

A PSI-BLAST comparison against online protein databases^[12] revealed that the two MoSto subunits are related to a family of uridine monophosphate kinases, enzymes that catalyze the reaction $\text{ATP} + \text{UMP} \rightarrow \text{ADP} + \text{UDP}$ (ATP = adenosine triphosphate, UMP = uridine monophosphate, ADP = adenosine diphosphate, UDP = uridine diphosphate). In fact, from a closer inspection of the sequences it turned out that the amino acid residues 77–82 of the α subunit and 75–80 of the β subunit (indicated by arrows in Figure 3) resemble the P-loop motif^[13] of an ATP-binding site.

The protein database check also showed that the *Azotobacter* MoSto is probably not as unique as hitherto believed. The

α	1	MTDITNSIKHVISETLARQITLQDRDLTRPVAGKRPIRLLPWLQVVKIGCR·VMDRGA
β	1	MANSTAELEELLMORSLTDPQLQAAAAAADFRLLPDAIVKIKGGQSVIDRGR
α	56	DAITLPLVEELRKLLEPHRLILITGACVRRARHVFVSVGLDLGLEVCGSLAPLAASEAGQ
β	54	AAVYPLVDEITVAARKNHKLLICTGACVRRARHLYSIAAGLGLPACVLAQLGSSVADQ
α	112	NGHILAAMLASECVSYVEHPTVADQLAIHLSATRAVVGSAFPPYHHHEFPGSR··I
β	110	NAAMLGQLLAKHGLIPVVGAGLS·AVPLSLAEVNAVVFSGMPPYKLMWRPAAEGVI
α	166	PPHRADTCATLLADAFGAAGLTIIVENVDCIYTADPNPDRGQARELPETSATDL·A
β	165	PPYRTDAGCFLLAEQFGCKQMI FVKDEDGLYTANE··KTSKDATEIPERISVDEMKA
α	221	KSEGPLPVDRALLDVMTARHIERVQVNVGLVPGRLTAALRGEHVGTILRTGVRPA
β	219	KGLHDSILEFPVLDLILQSAOHVREVVQVNVGLVPGNLTRALAGEHVGTIITAS

Figure 3. Sequence alignment between the α and β MoSto subunits as translated from the *Azotobacter* genome. Black boxes indicate identical amino acid residues, while grey boxes indicate those which are chemically similar and may fulfil a comparable function in proteins. The starting methionines of the subunits are not present in the functional protein. The sequence regions which represent the potential ATP-binding sites (P-loop motifs) are indicated by the arrows.

recently sequenced genome of *Rhodospseudomonas palustris*^[14] contains two adjacent genes (*rpa1441* and *rpa1442*) coding peptide chains that are 273 and 270 amino acids long and that are each more than 80% identical with the respective *A. vinelandii* MoSto subunits. The similarities are so striking that we feel it fairly safe to predict that the product of those genes is a functional and structural homologue of *A. vinelandii* MoSto. Another closely related peptide of 318 amino acids, which is coded by a plasmid gene (*pRhico094*) from *Azospirillum brasilense*,^[15] exhibits 86% identity with the *A. vinelandii* MoSto β subunit in an overlap that is 251 amino acids long.

Regulation of MoSto

Growth experiments with *A. vinelandii*, followed by electrophoretic examination of crude cell-free extracts confirmed the statement of Pienkos and Brill^[3] that MoSto is not coregulated with nitrogenase, but is synthesized constitutively, independent of the nitrogen source. It was formed in nitrogen-fixing *A. vinelandii* cells as well as in cells grown under nitrogenase-repressing conditions in the presence of ammonia. However, we found that, with respect to molybdenum, MoSto is coregulated with the conventional Mo nitrogenase. Mo has been determined to be an absolute requirement for expression of the structural genes of this nitrogenase system in *A. vinelandii*.^[16] In the case of the Mo storage protein, the existence of Mo regulation has been denied,^[3] which is probably due to the fact that this regulation occurs at nanomolar concentrations. Commercially available chemicals used in growth media

are often contaminated with Mo amounts sufficient to exceed such low concentrations. Having carefully removed Mo from the nutrient solutions to a concentration of <0.1 ppb (see the Experimental Section), we were able to follow the Mo-induced formation of the storage protein.

MoSto was quantitatively assayed by using Western immunoblot analysis. No MoSto could be detected in cells grown in Mo-depleted medium (Figure 1B, lane 1). In the range of 1–50 nM molybdate, the intensity of the MoSto bands increased significantly (Figure 1B, lanes 2–5). At concentrations higher than 50 nM molybdate, the MoSto content of the cells remained almost unchanged.

The Mo core

In order to structurally characterize the Mo sites, Mo–K-edge X-ray absorption spectroscopy (XAS) data were collected on a frozen solution of MoSto. Figure 4 displays the EXAFS and corresponding Fourier transformed spectra of MoSto (detailed fit results are given in the Experimental Section, Table 2, and Figure 8). As indicated by the vertical dashed lines, contributions of neighboring Mo atoms at $r(\text{Mo}\cdots\text{Mo})=3.27$ Å and at $r(\text{Mo}\cdots\text{Mo})=3.42$ Å were identified. Shells of back-scattering contributions with shorter distances were attributed to oxygen ligands (2 oxygen atoms each at 1.72, 1.91, and 2.28 Å). These results clearly proved that the MoSto sample contained a molybdenum–oxide cluster.

Does it follow from this conclusion that the detected cluster is bound to the protein? From the chemical point of view (see

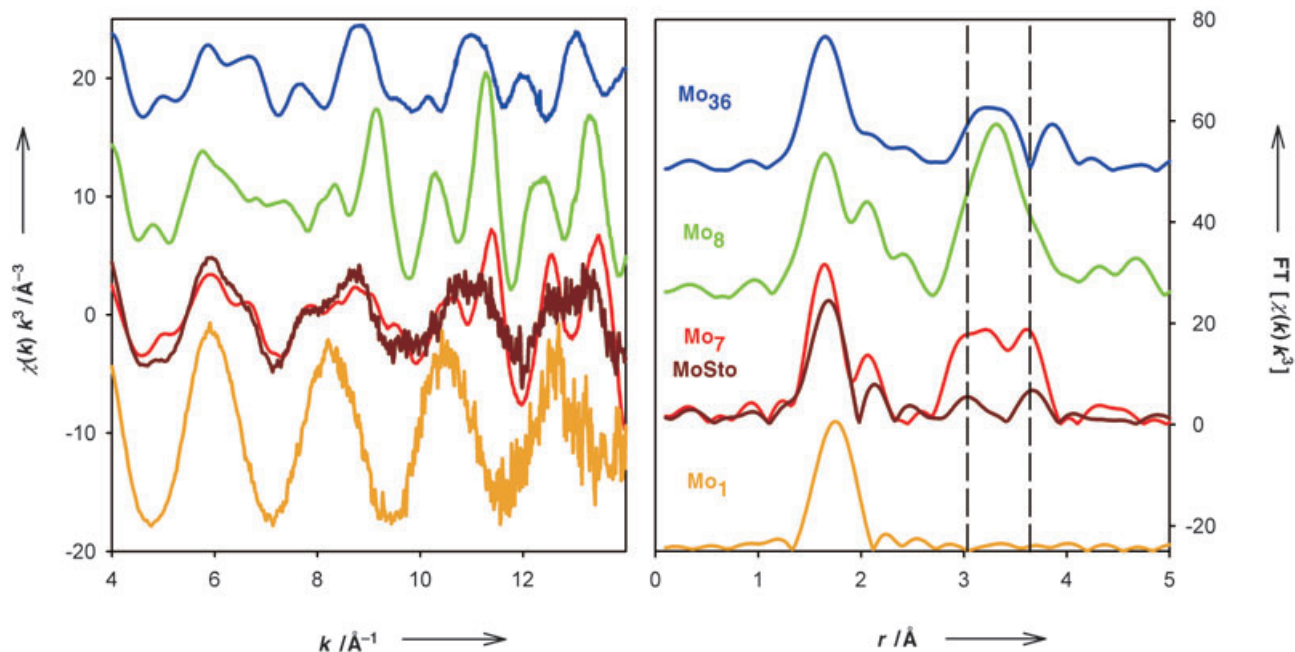


Figure 4. Measured Mo–K-edge EXAFS (left) and Fourier transform (right) results for MoSto (brown) in comparison to the spectra of salts of heptamolybdate (Mo_7 , red), octamolybdate (Mo_8 , green), $[\text{Mo}_{36}\text{O}_{112}(\text{H}_2\text{O})_{16}]^{8-}$ (Mo_{36} , blue), and a sodium molybdate solution (Mo_1 , yellow). Dashed vertical lines in the Fourier transform results indicate coinciding Mo...Mo back-scattering contributions for MoSto and Mo_7 , only. The refined spectra of MoSto and Mo_7 with the corresponding EXAFS parameters are given in the Experimental Section (Figure 8). Vertical offsets were applied for the spectra of Mo_1 , Mo_8 , and Mo_{36} and the Fourier transform results of Mo_1 , were scaled by 0.5 for better comparison. Abbreviations: χ = EXAFS amplitude, k = photoelectron wave number, r = distance (phase-corrected for first shell of back-scattering atoms), FT = Fourier transform amplitude.

the literature on the formation of polyoxomolybdates^[17], it is unlikely that such a cluster will be present in solution under the conditions used in our experiments. We performed a control EXAFS experiment by using a 3 mM disodium molybdate solution in 3-morpholino-propanesulfonic acid (MOPS) buffer (50 mM, pH 6.5), that is, exactly the same conditions as in the MoSto sample, but without the protein. In fact, only the monomeric molybdate $[\text{MoO}_4]^{2-}$ was identified (4 oxygen atoms at 1.77 Å; Figure 4, yellow curve) and no clusters had been formed. This result conclusively confirmed that the cluster detected in the MoSto sample must be protein-bound.

To further characterize the structure of this cluster, the spectra of three putative model systems were compared with the MoSto spectrum: tetraethylammonium β -octamolybdate (Mo_8 ; Figure 4), ammonium heptamolybdate (Mo_7 ; detailed fit results are given in the Experimental Section), and $\text{K}_8[\text{Mo}_{36}\text{O}_{112}(\text{H}_2\text{O})_{16}] \cdot 32\text{--}40\text{H}_2\text{O}$ (Mo_{36}). These compounds represent the most common iso-polymolybdate(vi) species in aqueous solution (at pH 1–7 and with a molybdate concentration of 0.01–1 M).^[17] Of these compounds Mo_7 has been found to exhibit the most structural similarity to the cluster present in MoSto (Figure 4; a direct comparison of the EXAFS parameters of MoSto and Mo_7 is given in Figure 8 and Table 2): It is evident that the EXAFS spectra of Mo_7 and MoSto are in phase over the entire data range. Furthermore, both signals share common spectral features, such as the double peak in the Fourier transform traces at approximately 34 Å, which originates from Mo back-scattering atoms (see the dashed vertical lines in Figure 4). It should be noted that, in contrast, this spectral region differs considerably from the spectrum with Mo_{36} , where further Mo–Mo contributions are present, as well as from that with Mo_8 (two upper spectra of Figure 4). In addition, multiple scattering contributions can be identified for Mo_8 ($k = 6\text{--}8\text{ \AA}^{-1}$ in the EXAFS spectrum) that are not present in the other samples.

Moreover, resolved double maxima in the EXAFS spectra of Mo_7 (for example, $k = 11$ and 13 \AA^{-1}) correspond to plateaux in the MoSto fine structure. However, the lower resolution of spectral details in the EXAFS spectra and the smaller Fourier transform amplitude for MoSto compared to Mo_7 suggest much larger structural disorder of the metal–oxide cluster bound to the storage protein. Disorder could originate from 1) a higher mobility in protein solution (before freezing) compared to solid heptamolybdate, 2) the presence of spatially more extended clusters compared to heptamolybdate, or 3) the coexistence of slightly different kinds of clusters in the protein solution.

Binding and release of Mo

The reaction conditions required for the processes of Mo release from and rebinding of Mo to the storage protein were studied with crude extracts as well as with the purified protein, both from cells grown with NH_4^+ , that is, under conditions of strict repression of *nif*-encoded proteins, including the MoFe nitrogenase protein and all proteins involved in the FeMo co-factor biosynthesis. Under such conditions, the storage protein

proved to be the predominant Mo-containing protein in *A. vinelandii* cells,^[5] so that even in the extracts the Mo-release/binding processes could be followed without significant disturbance by other Mo proteins. The results of the study strongly indicate the occurrence of unique biological mechanisms:

- 1) Regardless of whether extracts or samples of purified storage protein are used, the Mo release follows a pH-regulated “switch on” mechanism within a very narrow range. Whereas at pH 6.5–7.0 the Mo-containing holoprotein is stable, molybdenum is released (as molybdate) above pH 7.1, and at pH 7.6 the release is quantitative (Figure 5). The degree

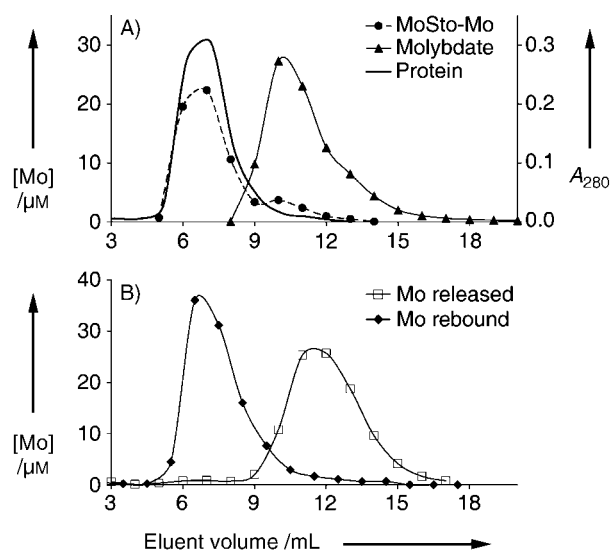


Figure 5. Sephadex G-25 gel filtrations of the molybdenum storage protein at different pH values in the presence (1 mM) and absence of ATP. The protein was homogeneously purified, samples were pretreated, and column runs were carried out as described in the Experimental Section. A) MoSto-Mo: Mo-elution profile of an untreated MoSto sample at pH 6.5 (protein-bound Mo as reference); Molybdate: Mo-elution profile of a molybdate solution sample (low-molecular-weight reference); Protein: protein-elution profile obtained by measuring the absorption of the fractions at 280 nm, average of all three runs with MoSto. B) Mo released: Mo-elution profile after pretreatment and column run of the sample at pH 7.6 in the absence of ATP; Mo rebound: Mo-elution profile after pretreatment of the sample at pH 7.6 in the absence of ATP (Mo release), a second treatment at the same pH value but in the presence of ATP (Mo rebinding), and subsequent column run.

and velocity of the Mo release is certainly also influenced by the temperature, incubation time, and protein concentration. (Detailed data on these aspects will be published elsewhere.) The key condition triggering the mechanism of Mo release is, however, the slight shift from neutral to weakly alkaline pH values. This is, in principle, in line with observations made in the field of polyoxomolybdate chemistry. In aqueous solutions increasing pH values lead to degradation of larger species into smaller.^[18] This process is, however, reversible, while in MoSto the Mo release cannot be reversed by simply lowering the pH value to <7.1 again.

- 2) “Binding of Mo” to the apoprotein, which involves the biosynthesis and insertion of the Mo–oxide-based cluster into the protein, requires ATP (or a related nucleotide) in a pro-

cess that is pH-independent (in the range 6.5–8.0). Mo, once released from the protein at weakly alkaline pH values, becomes reincorporated only in the presence of ATP (Figure 5). The role of ATP is in accordance with amino acid sequence data which indicate that MoSto might contain an ATP-binding site (see above). An earlier study had already shown that the exchange of MoSto-bound tungsten and free molybdate required a nucleotide (ADP or ATP); however, the exact role of ATP remained unclear with regard to whether it enabled the release of tungstate or led to the binding of molybdate.^[19]

Since both the release and binding of Mo function not only with cell-free extracts but also with highly purified storage protein, it can be concluded that none of these processes is dependent on the presence or involvement of other proteins such as Mo acceptor/transfer protein(s) or accessory protein(s) with insertase and/or chaperone functions, respectively.

The biosynthesis of the Mo–oxygen cluster in MoSto is a fascinating problem connecting aspects of both metalloprotein biochemistry and inorganic cluster chemistry. In the case of ferritin, the formation of the Fe–O core involves the oxidation $\text{Fe}^{\text{II}} \rightarrow \text{Fe}^{\text{III}}$ and subsequent condensation processes.^[7] In contrast, a redox process for the formation of the polynuclear metal core in MoSto is unlikely. From the point of view of inorganic molybdate chemistry and particularly from the experience with the recently synthesized giant Mo–O clusters which are the largest structurally characterized laboratory-made discrete species in inorganic chemistry,^[20–22] four factors are known to promote significant cluster growth: 1) low pH value, 2) high molybdate concentration, 3) the presence of certain other (ionic) template-type species which initiate the formation of a large number of different basic building units, and 4) partial reduction of Mo^{VI} to Mo^{V} . In the case of MoSto, factors 1 and 4 can be dismissed: due to its high number of exchangeable protons, a soluble cytoplasmic protein is not likely to provide an efficient barrier to sustain a pH gradient, while, on the other hand, a partially reduced $\text{Mo}^{\text{V}}\text{–O}$ cluster would be intensely blue and MoSto does not show significant absorption in the visible spectrum (data not shown). Additionally, the presence of Mo in a reduced state would correspond to a *K*-absorption edge position at lower energy in the XAS spectrum as compared to molybdate(vi). However, our XAS results indicate only the presence of Mo^{VI} centers in the protein (data not shown). On the other hand, factors 2 and 3 provide feasible conditions: the molybdate might be ATP-dependently transported into the protein, where aggregation would occur immediately due to the high local concentration, that is, under so-called confined geometries, and where the anionic Mo–oxide-based cluster(s) could finally be stabilized by positively charged amino acid side chains.

In this context it would be a challenge to investigate whether new clusters could be created biosynthetically, either in a protein modified by site-directed mutagenesis, that is, by exchanging an amino acid in the vicinity of the clusters, or by exposing the MoSto apoprotein to different oxometalates. The fact that the MoSto core is metal–oxide-based may even be

the starting point for links to research on molybdenum oxides, which play a major role in materials science and catalysis.^[23]

Conclusion

Based on protein-structure characteristics and the type of Mo compound present in the protein, molybdoproteins can be divided into five classes (Figure 6):

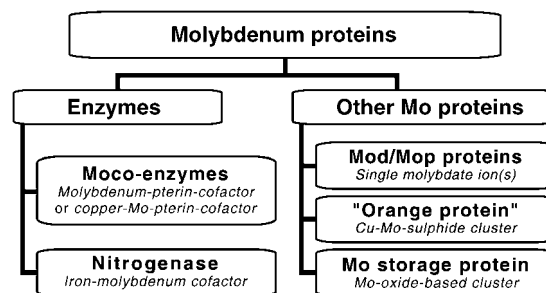


Figure 6. Classification of Mo-containing proteins according to the structure of the Mo component.

- 1) Mo nitrogenases contain a polynuclear iron–molybdenum cofactor (FeMoco) of $\text{Fe}_7\text{S}_9\text{MoN}$ /homocitrate composition.^[24]
- 2) Several types of oxidases, dehydrogenases, and hydroxylases contain an Fe-free molybdenum cofactor (Moco) composed of an organic pterin component and a mononuclear molybdenum–oxide fragment (an Mo atom bound to O and S atoms).^[25] An exceptional position is taken by the carbon monoxide dehydrogenase from *Oligotropha carboxidovorans*. This enzyme contains a binuclear $[\text{CuMo}(\text{=O})_2]$ cluster in which the Mo atom of the Moco is linked to copper through a sulphide bridge.^[26]
- 3) Molybdate-binding proteins (Mod/Mop proteins, “molbindins”) are involved in Mo transport, intracellular transfer, homeostasis, and gene regulation. These proteins contain up to eight molybdate ions (for example, ModG of *A. vinelandii*).^[2]
- 4) The small “orange protein”, so far the only representative of this class of molybdoproteins, has been detected in *Desulfovibrio gigas*, is of unknown function, and has been proposed to contain a pterin-free trinuclear molybdenum–copper sulphide cluster in a linear $[\text{S}_2\text{MoS}_2\text{CuS}_2\text{MoS}_2]$ arrangement.^[27]
- 5) The Mo storage protein of *A. vinelandii*, characterized in this work, represents a completely new type of molybdoprotein. This conclusion is based on several outstanding properties which differ fundamentally from those of all other known Mo-containing proteins:
 - a) MoSto can take up at least 90 Mo atoms per protein molecule.
 - b) The EXAFS spectroscopy results clearly prove that MoSto contains a Mo–oxide aggregate that is structurally related to the well-known heptamolybdate. Regardless of whether this aggregate may be present in the protein as a large single cluster or in the form of several smaller ones, it represents an unprecedented structure of a Mo

compound incorporated in a protein. Furthermore, MoSto is the only known noniron metal storage system with a metal-oxide-based core.

- c) The storage protein is much larger and more complex than the conventional molybdate-binding proteins. Its quaternary structure appears to be octameric, probably present as an $(\alpha_2\beta_2)_2$ arrangement.
- d) The amino acid sequence of MoSto does not show any similarity with sequences of other molybdoproteins. It revealed, on the other hand, that MoSto is related to a family of nucleotide monophosphate kinases which has hitherto been unknown in connection to Mo.
- e) Both the ATP-dependent Mo-binding and the pH-regulated Mo-release processes in the storage protein appear to follow unique biological mechanisms.

The Mo storage protein is not an exclusive feature of the genus *Azotobacter*, as hitherto assumed. MoSto genes have been shown also to occur in *Rhodospseudomonas palustris*, and with the rapidly increasing data on microbial genomes this storage system might also be found in a number of other nitrogen-fixing bacteria.

Experimental Section

Bacterial growth: The bacterial strain used in this study was *A. vinelandii* wild-type strain OP (DSM 366; ATCC 13705). The cells were grown under aerobic conditions in a modified Burk medium.^[28] Nitrogenase synthesis was strictly repressed by adding 20 mM ammonium acetate to the medium. Main cultures (600 mL in 2-L flasks) were incubated in a rotary shaker at 32 °C for 24 h up to an optical density (E_{436}) of 12–14. The cells were harvested by centrifugation and the resulting pellet was stored at 20 °C.

Mo-regulation experiments: Cells applied for Mo-regulation experiments were precultured twice in Mo-depleted growth medium and subsequently used for inoculation of the main cultures (100 mL of Mo-depleted medium in 300-mL flasks) which were supplemented with different amounts of molybdate. Effective Mo depletion of the growth medium (removal of Mo impurities from chemicals) was achieved by incubation of the medium with Mo-starved resting cells of *A. vinelandii* according to the method of Schneider et al.^[4] Cells from the late logarithmic growth phase were harvested and extracts prepared with lysozyme as described earlier.^[5] The cell-free extracts were finally subjected to Western immunoblot analyses (see below).

Protein purification: MoSto was kept in a buffer solution of MOPS (50 mM, pH 6.5) during the entire purification procedure. The harvested *Azotobacter* cells, suspended in the standard MOPS buffer, were disrupted in an Aminco-French pressure cell at 90 MPa. To remove unbroken cells, cell debris, and membrane particles, the resulting extract was centrifuged at 4 °C for 30 min at 80 000g. The supernatant is referred to as the crude extract.

The cell-free extract was loaded on a DEAE-Sephacel column (2.5 × 13 cm). The column was washed with 50 mM NaCl in MOPS buffer (50 mL) then eluted with a linear NaCl gradient (200 mL, 50 → 250 mM). MoSto was eluted at approximately 110 mM Cl⁻.

The combined MoSto peak fractions were subjected to a 40–50% ammonium sulphate fractionation. The precipitated MoSto was re-

dissolved in MOPS buffer, loaded on a Superdex 200 gel filtration column (2.5 × 60 cm) and eluted with the same buffer.

Analytical methods: Standard molybdenum assay: The catalytic method invented by Pantaler was used as described.^[29] The experimental scale was reduced by a factor of 10 so that the reaction could be carried out in standard 3-mL cuvettes. Prior to the assay, samples in gas-tight vessels were placed in a boiling water bath for 15 min, cooled to room temperature, and centrifuged to remove precipitated protein.

ICP-MS analyses: For higher accuracy and as a control for the catalytic routine assay, the level of Mo was also determined in some samples by mass spectrometry with inductively coupled plasma (ICP-MS), by using a Perkin-Elmer/Sciex ICP-QMS Elan 6000 instrument.

Protein determination: The protein content was determined by using the bicinchoninic acid method.^[30]

Polyacrylamide gel electrophoresis: The purity of protein components and molecular masses of the subunits were routinely analyzed by Tris/glycine SDS-PAGE, according to the method of Laemmli.^[31] The protein samples were supplemented with dithioerythritol (20 mM) prior to their denaturation. The stacking gel contained 4.8% (w/v) acrylamide and 0.13% (w/v) bisacrylamide cross-linker, whereas the resolving gel comprised 12.5% (w/v) acrylamide and 0.33% (w/v) bisacrylamide.

Western immunoblot analysis: Rabbit antisera containing monospecific polyclonal immunoglobulin G (IgG) antibodies directed against purified MoSto were employed in the immunoassays. Western immunoblot experiments were conducted according to the procedure described by Siemann et al.^[32] and principally based on the method of Towbin et al.^[33]

Experiments on Mo-binding and -release mechanisms: Cell-free extracts were prepared as described earlier^[5] and homogeneously purified storage protein was prepared as described above. While purified protein samples were directly used for Mo-binding/release experiments, the cytoplasmic fraction of the crude extract was first subjected to the following treatment: the extract solution was precipitated by ammonium sulphate (>80% saturation) in order to remove $[\text{MoO}_4]^{2-}$, ATP, and other low-molecular-weight species, then the pellet was washed twice with >80% saturated $(\text{NH}_4)_2\text{SO}_4$ and redissolved in MOPS buffer (50 mM, pH 6.5). Aliquots of this solution (1.5 mg of protein per mL) or of the solution of the purified protein (2 mg per mL) were taken and the pH value was adjusted to the required value. Samples for "Mo-release experiments" were then incubated for 1 h at 30 °C, subsequently loaded onto a Sephadex G-25 gel filtration column, and eluted with MOPS buffer (50 mM) at a pH value identical to that of the sample. In the case of "Mo-binding experiments", the sample was divided into two halves after the 1 h incubation (30 °C). One half was subjected to Sephadex G-25 gel filtration to ascertain that Mo had really been released completely from the protein after this incubation period (control run). ATP and MgCl_2 (1 mM each) were added to the other half (which had not been gel-filtrated) and the sample was left for a second incubation period under the same conditions. Finally, this latter sample was gel-filtrated on Sephadex G25. The elution buffer contained ATP at the same concentration as the sample itself. The resulting fractions (1 mL each) were analyzed for Mo and protein content.

SAXS investigations: For SAXS analysis, the peak MoSto fractions from gel filtration were combined and concentrated 15-fold in an Amicon B15 concentrator. The concentrated solution (correspond-

ing to the sample applied to the SDS gel in lane 5 of Figure 1 A) was centrifuged and the supernatant (protein content 17 g L^{-1}) was used to prepare a set of samples with different protein concentrations (see below) by diluting with MOPS buffer. Dithiothreitol was added to each sample (final concentration 10 mM) in order to prevent oxidative degradation of the protein during measurement.

SAXS data on MoSto solutions were collected at the European Molecular Biology Laboratory (EMBL) X33 beam-line on the storage ring DORIS at Deutsches Elektronensynchrotron (DESY), Hamburg, Germany,^[34] at a wavelength, λ , of 0.15 nm and at ambient temperature. A linear-delay line-readout proportional gas detector^[35] was used to record the scattering patterns in time frames of one minute. Data reduction including normalization to the intensity of the primary beam and the protein concentration, correction for the detector response, and subtraction of the scattering from the buffer was done by using the program SAPOKO.^[36] The scattering curves $I(s)$ versus s ($s_{\text{max}} = 2 \sin \theta_{\text{max}} / \lambda = 0.5 \text{ nm}^{-1}$; s = scattering vector; 2θ = scattering angle) for three different protein concentrations (3.75 , 10 , and 13 g L^{-1}) were averaged for further data analysis. The molecular mass of MoSto was determined from the extrapolated forward scattering $I(0)$ with an uncertainty of approximately 10% by using a solution of bovine serum albumin with known concentration as the reference. The shape was calculated *ab initio* with the chain-compatible dummy residues approach.^[37] Input data consisted of the distance distribution obtained from the averaged scattering data by using the program GNOM^[38] as well as the number of amino acid residues ($\alpha_4\beta_4$) from Figure 3. Figure 2 displays the best structure obtained from 20 independent calculations; the theoretical scattering curve and distance distribution corresponding to this structure are compared with the experimental data in Figure 7. The 20 structural models were compared pairwise

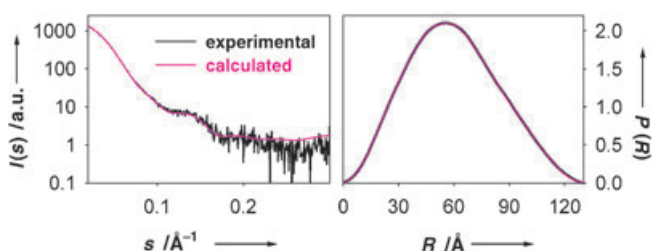


Figure 7. Averaged X-ray scattering curve (left) and corresponding distance distribution function (right) for MoSto. Experimental data are represented as black curves; the calculated curves (dark red) correspond to the model shown in Figure 2. Abbreviations: $I(s)$ = scattering intensity, s = scattering vector, $P(R)$ = distance distribution, R = distance, a.u. = arbitrary units.

in terms of distance root mean square deviation (rmsd) or normalised spatial discrepancy (NSD) value.^[39] The structure with the smallest average distance rmsd from all other structures in the set of 20 calculations was considered to be the best. Deviations from the best structure were typically in the range of 5 Å (distance rmsd).

EXAFS investigations: XAS data were collected at the EMBL bending magnet EXAFS beam-line D2, DESY, Hamburg, Germany, with an Si(311) double-crystal monochromator, a focusing mirror, and a set-up for absolute energy calibration.^[40] The samples were mounted in a two-stage Displex cryostat and kept at about 25 K . The X-ray absorption of the MoSto sample was recorded as a $\text{Mo}_{K\alpha}$ fluorescence excitation spectrum by employing a Canberra 13-element solid-state detector. Solid model compounds were observed in the

absorption mode. Data reduction and analyses of the EXAFS of Mo–K-edges (an edge position of 20002 eV was assumed) were achieved with the EXPROG program package^[41] and the refinement program EXCURV98,^[42] respectively. Experimental XAS data and fits for MoSto and Mo_7 (EXAFS and Fourier transform) are shown in Figure 8; corresponding parameters appear in Table 2.

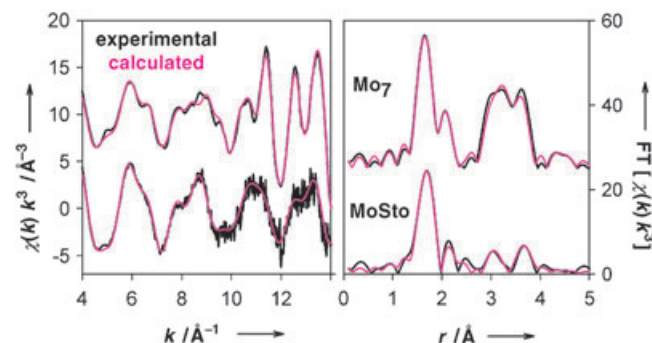


Figure 8. Mo–K-edge EXAFS (left) and Fourier transform (right) results for MoSto (experimental: black, calculated: dark red) in comparison to the spectrum of heptamolybdate (Mo_7 , experimental: black, calculated: magenta). EXAFS parameters of the calculated spectra are given in Table 2.

Table 2. EXAFS parameters^[a] for MoSto and $[\text{Mo}_7\text{O}_{24}]^{6-}$. The corresponding spectra are shown in Figure 8.

Sample	Atom	$N^{[b]}$	r [Å^{-1}]	$2\sigma^2$ [Å^2]	E_0 [eV]	R [%]
MoSto	O	2	1.722(3)	0.003(1)	−9.7(12)	27.4
	O	2	1.908(11)	0.021(4)		
	O	2	2.279(20)	0.030(8)		
	Mo	1.7	3.274(7)	0.009(1)		
$[\text{Mo}_7\text{O}_{24}]^{6-}$	Mo	1.7	3.422(7)	0.007(1)	−11.3(6)	12.9
	O	2	1.721(2)	0.003(1)		
	O	2	1.933(3)	0.006(1)		
	O	2	2.201(6)	0.019(2)		
	Mo	1.7	3.230(2)	0.005(1)		
	Mo	1.7	3.407(2)	0.003(1)		
	Mo	0.6	4.296(10)	0.010(2)		
	Mo	0.6	5.409(13) ^[c]	0.006(3)		
Mo	0.6	5.675(13) ^[c]	0.009(3)			

[a] N = number of back-scattering atoms, r = distance, $2\sigma^2$ = Debye–Waller parameter, E_0 = energy correction (see manual of EXCURV98^[42]), R = R factor (reflects the goodness of the fit; see ref. [42]). Values in parentheses correspond to the numerical uncertainty of the last digit (twice the standard deviation). As the typical precision for distance determination is 0.01 – 0.02 Å , only two digits are given in the Results section of the paper. [b] Coordination numbers were fixed at the average values in heptamolybdate. Due to nonequivalent Mo sites, the coordination numbers are rational values. [c] Distances larger than 5 Å are not shown in Figure 8 but were included in the fit.

For the EXAFS experiments, a protein sample of the preparation obtained from the ammonium sulphate fractionation step (50% saturated precipitate) was used. Even if this preparation was not yet homogeneous ($\approx 70\%$ purity; see lane 4 in Figure 1 A), it proved to have an excellent quality for the EXAFS study. Careful Mo analyses of all gel filtration fractions had shown that the Mo storage protein was the only detectable Mo protein present in the ammonium sulphate fraction used. Since EXAFS analysis is an element-specific technique, Mo-free components of the sample do not interfere with the Mo EXAFS signal. Before application, the precipitated

MoSto was redissolved in MOPS buffer (50 mM, pH 6.5) and passed over a Sephadex G-25 column to remove ammonium sulfate, chloride, and non-protein-bound Mo. This MoSto solution (75 μL ; total protein content 15 g L^{-1} ; Mo concentration 2.5 mM, that is, approximately 55 Mo atoms per protein molecule) was placed into sample cells of plexiglass covered with polyimide windows. Reference samples were prepared by mixing each of the model compounds, heptamolybdate (40 mg), octamolybdate (40 mg), and $[\text{Mo}_{36}\text{O}_{112}(\text{H}_2\text{O})_{16}]^{8-}$ (30 mg), with boron nitride (100 mg) in order to avoid thickness effects.^[43] The mixtures were pasted homogeneously into sample cells similar to that used for the protein solution.

Origin of the reference compounds used for EXAFS measurements: Analytical grade ammonium heptamolybdate was purchased from Merck (Germany). Tetraethylammonium- β -octamolybdate was prepared as described by Fuchs et al.^[44] $\text{K}_8[\text{Mo}_{36}\text{O}_{112}(\text{H}_2\text{O})_{16}] \cdot 32\text{--}40\text{H}_2\text{O}$ was prepared as described by Krebs and Paulat-Böschchen.^[45] The identity of the synthesized products was confirmed by determining the unit-cell dimensions with single-crystal X-ray diffraction.

The protein sequence data reported in this paper will appear in the Swiss-Prot and TrEMBL knowledgebase under the accession numbers P84308 and P84253.

Acknowledgements

This research project was supported by the Deutsche Forschungsgemeinschaft (DFG). M.G. acknowledges support by the German Ministry of Education and Research (BMBF) under contract no. 05SN8FLA7. The authors thank Michel Koch (EMBL Hamburg) for assistance with SAXS data collection and analysis as well as for critically commenting on the manuscript, Marc Niebuhr, Maxim Petoukhov, and Anna Sokolova (all EMBL Hamburg) for the introduction to SAXS data analysis, Malgorzata Korbas (EMBL Hamburg) for aid in preparing the SAXS- and EXAFS-related figures, and Bernd Masepohl (Ruhr-Universität Bochum) for advice and discussions.

Keywords: bioinorganic chemistry • metal storage protein • metalloproteins • molybdenum • polyoxomolybdate

- [1] R. N. Pau, W. Klipp, S. Leimkühler in *Iron and Related Transition Metals in Microbial Metabolism* (Eds.: G. Winkelmann, C. J. Carrano), Elsevier, Amsterdam, **1997**, pp. 1–13.
- [2] a) R. N. Pau, D. M. Lawson in *Metal Ions in Biological Systems, Vol. 39: Molybdenum and Tungsten: Their Roles in Biological Processes* (Eds.: A. Sigel, H. Sigel), Marcel Dekker, New York, **2002**, pp. 31–74; b) A.-K. Duhme, W. Meyer-Klaucke, D. J. White, L. Delarbre, L. A. Mitchenall, R. N. Pau, *J. Biol. Inorg. Chem.* **1999**, *4*, 588–592.
- [3] P. T. Pienkos, W. J. Brill, *J. Bacteriol.* **1981**, *163*, 743–751.
- [4] K. Schneider, A. Müller, K.-U. Johannes, E. Diemann, J. Kottmann, *Anal. Biochem.* **1991**, *193*, 292–298.
- [5] A. Müller, W. Suer, C. Pohlmann, K. Schneider, W.-G. Thies, H. Appel, *Eur. J. Biochem.* **1997**, *246*, 311–319.
- [6] R. H. Maynard, R. Premakumar, P. E. Bishop, *J. Bacteriol.* **1994**, *176*, 5583–5586.
- [7] N. D. Chasteen, P. M. Harrison, *J. Struct. Biol.* **1999**, *126*, 182–194.
- [8] O. Gakh, J. Adamec, A. M. Gacy, R. D. Twisten, W. G. Owen, G. Isaya, *Biochemistry* **2002**, *41*, 6798–6804.
- [9] H. Nichol, O. Gakh, H. A. O'Neill, I. J. Pickering, G. Isaya, G. N. George, *Biochemistry* **2003**, *42*, 5971–5976.
- [10] <http://www.azotobacter.org/blast.html>; search program "tblastn".
- [11] D. G. Gourley, A. W. Schüttelkopf, L. A. Anderson, N. C. Priest, D. H. Boxer, W. N. Hunter, *J. Biol. Chem.* **2001**, *276*, 20641–20647.
- [12] S. F. Altschul, T. L. Madden, A. A. Schaffer, J. Zhang, Z. Zhang, W. Miller, D. J. Lipman, *Nucleic Acids Res.* **1997**, *25*, 3389–3402.
- [13] M. Saraste, P. R. Sibbald, A. Wittinghofer, *Trends Biochem. Sci.* **1990**, *15*, 430–434.
- [14] F. W. Larimer, P. Chain, L. Hauser, J. Lamerdin, S. Malfatti, L. Do, M. L. Land, D. A. Pelletier, J. T. Beatty, A. S. Lang, F. R. Tabita, J. L. Gibson, T. E. Hanson, C. Bobst, J. L. Torres y Torres, C. Peres, F. H. Harrison, J. Gibson, C. S. Harwood, *Nat. Biotechnol.* **2004**, *22*, 55–61.
- [15] E. Vanbleu, K. Marchal, M. Lambrecht, J. Mathys, J. Vanderleyden, *FEMS Microbiol. Lett.* **2004**, *232*, 165–172.
- [16] F. Luque, R. N. Pau, *Mol. Gen. Genet.* **1991**, *227*, 481–487.
- [17] K.-H. Tytko, G. Baethe, E.-R. Hirschfeld, K. Mehmke, D. Stellhorn, *Z. Anorg. Allg. Chem.* **1983**, *503*, 43–66.
- [18] M. T. Pope, A. Müller, *Angew. Chem.* **1991**, *103*, 56–70; *Angew. Chem. Int. Ed. Engl.* **1991**, *30*, 34–48.
- [19] R. M. Allen, J. T. Roll, P. Rangaraj, V. K. Shah, G. P. Roberts, P. W. Ludden, *J. Biol. Chem.* **1999**, *274*, 15869–15874.
- [20] N. Hall, *Chem. Commun.* **2003**, 803–806.
- [21] A. Müller, P. Kögerler, C. Kuhlmann, *Chem. Commun.* **1999**, 1347–1358.
- [22] A. Müller, E. Beckmann, H. Bögge, M. Schmidtman, A. Dress, *Angew. Chem.* **2002**, *114*, 1210–1215; *Angew. Chem. Int. Ed.* **2002**, *41*, 1162–1167.
- [23] A. Müller, R. Maiti, M. Schmidtman, H. Bögge, S. K. Das, W. Zhang, *Chem. Commun.* **2001**, 2126–2127, and references therein.
- [24] O. Einsle, F. A. Tezcan, S. L. A. Andrade, B. Schmid, M. Yoshida, J. B. Howard, D. C. Rees, *Science* **2002**, *297*, 1696–1700.
- [25] K. V. Rajagopalan, J. L. Johnson, *J. Biol. Chem.* **1992**, *267*, 10199–10202.
- [26] a) H. Dobbek, L. Gremer, R. Kiefersauer, R. Huber, O. Meyer, *Proc. Natl. Acad. Sci. USA* **2002**, *99*, 15971–15976; b) M. Gnida, R. Ferner, L. Gremer, O. Meyer, W. Meyer-Klaucke, *Biochemistry* **2003**, *42*, 222–230.
- [27] a) G. N. George, I. J. Pickering, E. Y. Yu, R. C. Prince, S. A. Bursakov, O. Y. Gavel, I. Moura, J. J. G. Moura, *J. Am. Chem. Soc.* **2000**, *122*, 8321–8322; b) S. A. Bursakov, O. Y. Gavel, G. Di Rocco, J. Lampreia, J. Calvete, A. S. Pereira, J. J. G. Moura, I. Moura, *J. Inorg. Biochem.* **2004**, *98*, 833–840.
- [28] G. Strandberg, P. W. Wilson, *Can. J. Microbiol.* **1968**, *14*, 25–31.
- [29] R. P. Pantaler, *Zh. Anal. Khim.* **1963**, *18*, 603–609.
- [30] P. K. Smith, R. I. Krohn, G. T. Hermanson, A. K. Mallia, F. H. Gartner, M. D. Provenzano, E. K. Fujimoto, N. M. Goeke, B. J. Olson, D. C. Klenk, *Anal. Biochem.* **1976**, *150*, 76–85.
- [31] U. K. Laemmli, *Nature* **1970**, *227*, 680–685.
- [32] S. Siemann, K. Schneider, K. Behrens, A. Knöchel, W. Klipp, A. Müller, *Eur. J. Biochem.* **2001**, *268*, 1940–1952.
- [33] H. Towbin, T. Staehelin, J. Gordon, *Proc. Natl. Acad. Sci. USA* **1979**, *76*, 4350–4354.
- [34] M. H. J. Koch, J. Bordas, *Nucl. Instrum. Methods* **1983**, *208*, 461–469.
- [35] A. Gabriel, F. Dauvergne, *Nucl. Instrum. Methods* **1982**, *201*, 223–224.
- [36] P. V. Konarev, V. V. Volkov, A. V. Sokolova, M. H. J. Koch, D. I. Svergun, *J. Appl. Crystallogr.* **2003**, *36*, 1277–1282.
- [37] D. I. Svergun, M. V. Petoukhov, M. H. J. Koch, *Biophys. J.* **2001**, *80*, 2946–2953.
- [38] D. I. Svergun, *J. Appl. Crystallogr.* **1992**, *25*, 495–503.
- [39] M. B. Kozin, D. I. Svergun, *J. Appl. Crystallogr.* **2001**, *34*, 33–41.
- [40] R. F. Pettifer, C. Hermes, *J. Appl. Crystallogr.* **1985**, *18*, 404–412.
- [41] F. Nolting, C. Hermes, *EXPROG: EMBL EXAFS data analysis and evaluation program package*, **1992**.
- [42] H. N. Binsted, R. W. Strange, S. S. Hasnain, *Biochemistry* **1992**, *31*, 12117–12125.
- [43] E. A. Stern, K. Kim, *Phys. Rev. B* **1981**, *23*, 3781–3787.
- [44] a) J. Fuchs, I. Knöpnadel, I. Brüdgam, *Z. Naturforsch.* **1974**, *29b*, 473–475; b) J. Fuchs, I. Knöpnadel, *Z. Kristallogr.* **1982**, *185*, 165–179.
- [45] B. Krebs, I. Paulat-Böschchen, *Acta Crystallogr. Sect. B: Struct. Crystallogr. Cryst. Chem.* **1982**, *38*, 1710–1718.

Received: July 26, 2004

Published online: January 13, 2005